Rotman Lens-Based Wide Angular Coverage and High-Gain Semipassive Architecture for Ultralong Range mm-Wave RFIDs

Aline Eid, *Student Member, IEEE*, Jimmy G. D. Hester, *Student Member, IEEE*, and Manos M. Tentzeris, *Fellow, IEEE*

***Abstract*—In this letter, the authors demonstrate, for the first time, the implementation of a fully-flexible, energy autonomous Rotman lens-based backscattering RFID tag operating in the 28 GHz 5G band. The Rotman lens front end was designed, simulated, fabricated on a thin flexible substrate and its gain and differential radar cross section (RCS) tested. The structure displays a simultaneous high gain and wide angular coverage, resulting in a remarkable RCS, measured in both planar and severe bending conditions. A low power oscillator was then added to the retrodirective array to test its detectability as a backscatterer at an unprecedented range of up to 64 m while displaying a power consumption as low as 2.64 μW, effortlessly supplied by its flexible solar cell in normal office indoor conditions. Enabled by the implementation of a high degree of focalizing retrodirectivity, this unique Rotman lens-based system could enable the birth of RFIDs with practical reading ranges exceeding 1.8 km.**

***Index Terms*—5G, flexible electronics, Internet of Things (IoT), millimeter-wave (mm-wave), RFID, smart skin.**

I. Introduction

OUR era is witnessing revolutionary developments in the fields of millimeter-wave (mm-wave) and Internet-of-Things (IoT) technologies. The realization of low-power, high-gain, and orientation-agnostic tags is therefore highly desirable. One potential way of satisfying this goal is through the implementation of retrodirective arrays and beamforming networks (BFNs)-based RFID tags, which have been shown to enable extended reading ranges due to their focalization of the reflected signal [1]. Since power consumption is a major limitation, intelligent phased arrays are not an adequate solution. Retrodirective arrays passively reflect the impinging electromagnetic wave back—with gain—toward the direction of incidence. A very well-known rectrodirective design is the Van Atta reflectarray [2], where each antenna pair is connected with a transmission line of the same electromagnetic-phase length. Hester and Tentzeris [3] and Vitaz *et al.* [4] have demonstrated the successful implementation of mm-wave Van Atta arrays for the realization of ultralong range and large-coverage wireless sensors with electrically large tags. Although the Van Atta front end is a strong candidate for semipassive and chipless RFIDs, its use for passive systems is suboptimal [5]. This is due to the fact that the power received by the tag is inherently divided among the connecting lines, resulting in shorter turn-ON ranges if these were connected to rectifiers to power the tag. Moreover, the basic Van Atta structure is limited to amplitude modulation backscatter communications approaches unless made hybrid, resulting in more complex systems. For example, Alhassoun *et al.* [6] proposed a rat-race-based RFID tag that implemented a binary phase shift keying (BPSK) modulation scheme. Other techniques rely on altering the structure of the Van Atta array with costly switches to enable other modulation schemes such as quadrature-phase shift keying [7]. An alternative approach, proposed here, is to utilize BFNs, which are used to effectively create simultaneous beam angular coverage with large-gain arrays by mapping a set of directions to a set of feeding ports. A previous work had demonstrated that the Rotman lens—a passive type of BFNs that does not rely on any active circuitry—is the ideal candidate for mm-wave applications due to its design simplicity, ultralarge bandwidth, high gain and wide angular coverage [8]. Unlike the Van Atta array, if a wave impinges upon the array from a given direction, the Rotman lens-based array combines all the power received by all the antennas and focuses

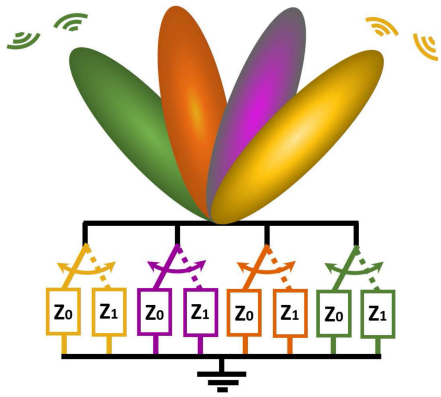

Fig. 1. Schematic representing the Rotman lens-based retrodirective backscatter front end.

Manuscript received March 29, 2020; revised May 29, 2020; accepted June 9, 2020. Date of publication June 16, 2020; date of current version November 23, 2020. This work was supported in part by the Air Force Research Laboratory and the NSF-EFRI. This work was performed in part at the Georgia Tech Institute for Electronics and Nanotechnology, a member of the National Nanotechnology Coordinated Infrastructure (NNCI), supported by the National Science Foundation under Grant ECCS-1542174. *(Corresponding author: Aline Eid.)*

The authors are with the School of Electrical and Computer Engineering, Georgia Institute of Technology, Atlanta, GA 30332 USA (e-mail: aeid7@gatech.edu; jimmy.hester@gatech.edu; etentze@ece.gatech.edu).

Digital Object Identifier 10.1109/LAWP.2020.3002924

it to a single beam port on the other side of the lens, opposite to the direction of the impinging signal, as shown in Fig. 1.

Therefore, since no RF power division is involved in the receiving scenario, the Rotman lens design presented in [8] enables optimal energy harvesting for passive RFIDs. If the Rotman lens structure could be enabled with backscattered communication capabilities, then the door for high beamwidth and high-gain fully passive RFIDs would be open. In addition to the advantage of RF combining, the lens is not limited to amplitude modulation schemes. Since the modulation of the reflection can be implemented by simply changing the load at all the beam ports as shown in Fig. 1, the implementation of all the techniques applied to traditional lower frequency RFIDs—including continuous spectrally efficient modulation [9]—can also be taken advantage of retrodirective antenna systems. In this letter, the authors demonstrate, for the first time, a full implementation of an entirely flexible, high-gain, and large-beamwidth Rotman lens-based retrodirective backscattering RFID system at mm-wave frequencies. With a power consumption in the order of 2.64 μW and a 1.2 V voltage requirement supplied by a solar cell, this system represents a breakthrough in the field of mm-wave backscattering systems, offering a theoretical maximum range of up to 1.8 km. This technology could be broadly utilized for applications ranging from ubiquitous environmental sensing for smart cities and smart agriculture (such as chemical analytes, humidity, moisture, temperature) to the tracking of items for logistics.

II. Components of the System

A. Single-FET Low-Cost mm-Wave Switch for Backscatter-Modulation

The proposed RFID tag aims for an operation in the mm-wave range, more specifically in the 28 GHZ 5G band. At those frequencies, finding a low-cost, low-power consumption switch becomes challenging. Fortunately, the super-low noise FET CE3520K3 from CEL is mm-wave compatible and fulfills the aforementioned characteristics. The FET switches between two different loads under zero biased and biased conditions. Before integration with the lens system, the switch was characterized by evaluating its magnitude and phase behavior for different source radial stubs lengths, selected to maximize the modulation factor defined in (1) which, for passive front ends, is always smaller than 1.

$$M = \frac{1}{4}|\Gamma_0 - \Gamma_1|^2 \tag{1}$$

where Γ_0 and Γ_1 are the reflection coefficients at the two extreme states of modulation. The switch schematic shown in Fig. 2 was printed on a flexible 180 μm thin liquid crystal polymer (LCP) substrate using an inkjet printing masking technique followed by etching. The *S*-parameters were measured using the VNA for gate-to-source voltages of 0 and -1.2 V. Fig. 2 shows a very adequate switching with a modulation factor of 0.12. It should be noted that larger modulation factors could be achieved using more expensive and complex mm-wave switches.

B. Rotman Lens-Based Retrodirective Array

The Rotman lens is a unique type of passive BFNs that relies on true-time-delays, which translate to ultrawideband operation [10]. This property differentiates the Rotman lens from any other type of passive BFNs such as the Butler or Blass matrices that operate over a much narrower frequency band. Just like an optical lens, the Rotman lens introduces differential propagation time delays to wavefronts impinging onto the various points of its surface. By properly tuning the shape of the lens, the number of antenna ports, beam ports, and dummy ports surrounding it, one could achieve a desired set of properties. The resulting structure maps a set of selected radiation directions to an associated set of beam-ports. The choice of the number of antenna and beam ports around the lens is governed by two fundamental parameters essential for high-performance retrodirective arrays: array factor and angular coverage. Structures with varying sizes were designed in Antenna Magus before being simulated in CST Studio Suite with the number of antenna ports and beam ports increased up to 64 and 48, respectively. The set resulting in the best compromise between a good array factor and large angular coverage comprised of eight antenna arrays and six beam ports. Dummy ports, that are common in the design of Rotman lenses for sidelobes suppression, were not added because the presence of sidelobes does not interfere with backscattering operation. Tapered lines were also added on both sides of the lens to create smooth impedance transitions from the antenna to the lens as well as from the lens to the beam ports.

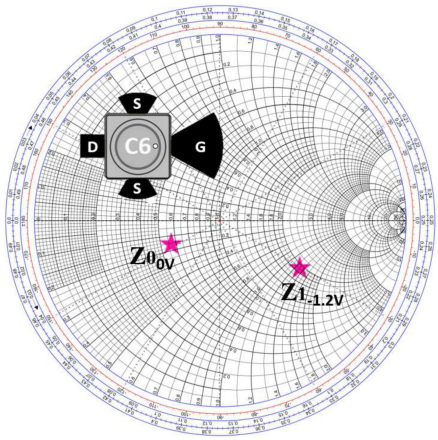

Fig. 2. Measured reflection coefficients of the mm-wave switch under $V_{GS} = 0$ V and -1.2 V.

Eight linear antenna arrays consisting of five serially fed rectangular patches—with vertical beamwidth of about 20° appropriate for most use cases, where environments expand mostly horizontally—were connected to the antenna ports, and the radiation properties of the lens-based antenna system were simulated and accurately measured at every port while all five remaining ports were terminated with a 50 Ω load to ensure the proper operation of the lens. A 20 dBi horn antenna was used to transmit power at 28.5 GHz to the lens antenna array that was precisely rotated in angular increments of 5°. Both simulated and measured gains are shown in Fig. 3, displaying very good similarity and demonstrating a measured gain of approximately 17 dBi and an angular coverage of around 110° in front of the lens, thereby validating the effective operation of the antenna array.

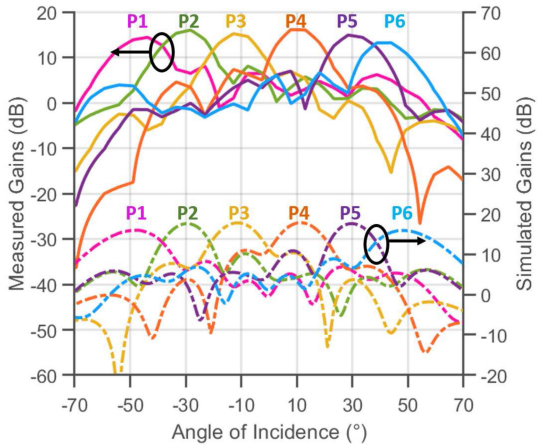

Fig. 3. Measured and simulated gain values at all six ports (P1–P6) of the Rotman lens-based antenna array.

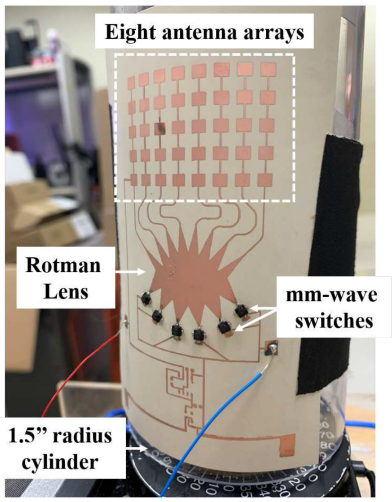

Fig. 4. Picture of the fabricated Rotman-lens-based retrodirective array placed on a 1.5″ radius cylinder.

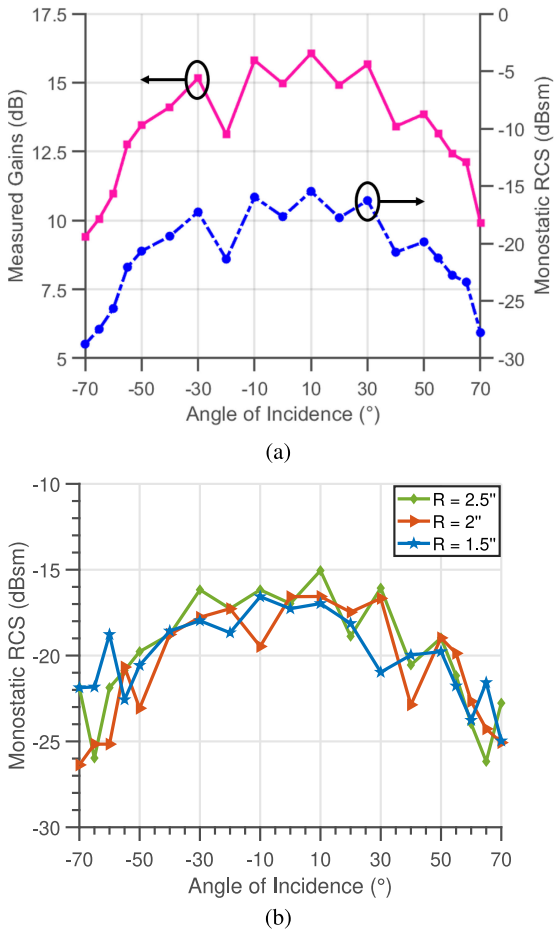

Fig. 5. (a) Plot of the measured monostatic differential RCS as well as the extracted gain of the planar structure. (b) Plot of the measured monostatic differential RCS for three different bending scenarios.

The next step consisted of evaluating the performance of the system as a switchable retrodirective array. For this purpose, six of the mm-wave switches presented in Section II-A were attached to the beam ports of the lens resulting in the structure shown in Fig. 4, printed on flexible copper-clad LCP substrate ($\varepsilon_r = 3.02$ and $h = 180\,\mu$m) using an inkjet-printed masking technique followed by etching.

The monostatic differential RCS of the Rotman lens-based retrodirective structure was measured using two colocated emitting and receiving horn antennas, while the array was placed on planar and bent surfaces and precisely rotated in angular increments of 5°. By controlling the biasing on the switches connected at the beam ports, the ON and OFF RCSs were measured and their difference was later calculated to extract the differential RCS of the structure. A 6-in-radius metal sphere was used as a reference target, for the accurate normalization of the RCS measurements. Fig. 5(a) displays the monostatic differential RCS as well as the associated gain of the Rotman lens-based retrodirective array placed on a planar surface. It should be noted that the calculated gain values take into account the modulation factor of the implemented switch as described in more details in [11]. The results of this test, measured at the optimal frequency of 28.5 GHz display a maximum RCS of -15.4 dBm, with a variation of less than 8 dB from $-60°$ to 60° of interrogation angle: the structure displays a high and largely isotropic differential RCS. It should be noted that a smoother differential RCS response could be achieved by increasing the number of beam ports on the Rotman lens resulting in less abrupt fluctuations with respect to the angle of incidence. The Rotman lens was then placed on cylinders with different bending radii—ranging from 1.5″ to 2.5″—to assess the effect of bending on the RCS behavior. Fig. 5(b) portrays the stability and robustness of this printed and flexible mm-wave Rotman lens prototype structure under bending with a measured variation of the RCS of less than 8 dB (equivalent to 4 dB in gain) over an angular coverage of 120°. The phase shift induced by bending the structure down to 1.5″ in radius was also calculated for a maximum angle of incidence of 60° using (9) presented in [1]. The maximum phase difference was found to be $\Delta\phi = 0.31\pi$, which is rather negligible and, therefore, supports the conclusion on the minor effect of bending on the array factor for bending radii down to below 1.5″.

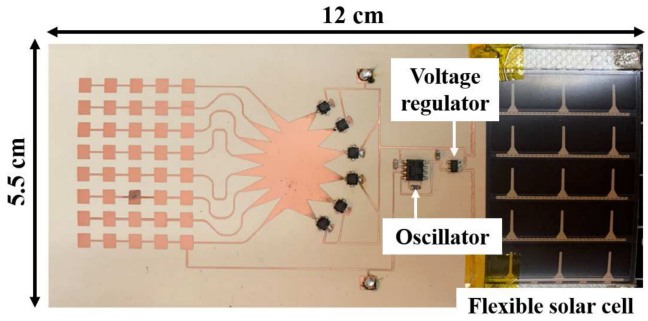

Fig. 6. Picture of the fully flexible power-autonomous Rotman-based semi-passive RFID tag proof-of-concept prototype. The overall dimensions are $5.5 * 12\,\text{cm}^2$.

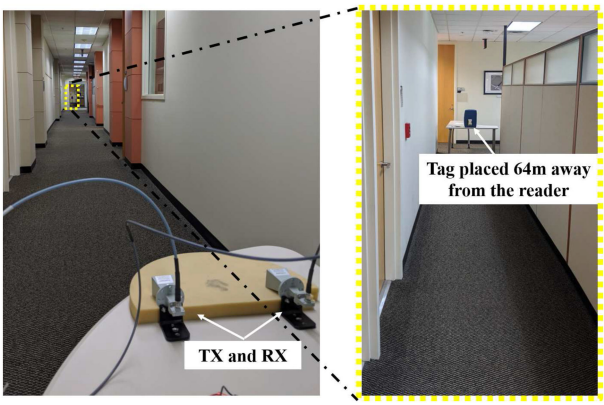

Fig. 7. Photograph of the setup and environment used to measure the Rotman lens-based tag long-range capabilities.

III. Fully Flexible Rotman-Lens-Based Semipassive RFID Tag

In the previous section, it was demonstrated that the Rotman lens can provide both high gain and wide angular coverage: two properties that justify its use as a retrodirective array for long-range mm-wave backscattering RFID applications. The fully flexible proof-of-concept prototype printed on thin LCP is shown in Fig. 6 and features the addition of a low-power oscillator (CSS555), a voltage regulator, and a flexible solar cell. The overall power consumption of the system was measured to be 2.64 μW, effortlessly supplied by the attached solar cell under normal-office indoor lighting conditions.

In order to test the system's long range communication capabilities, the tag was placed at various distances away from the reader while being illuminated by a 20 dB gain horn antenna supplied with a signal generated with a transmitted power of 28 dBm at 28.5 GHz, yielding an effective isotropic radiated power (EIRP) of 48 dBm. The receiving channel used another 20 dB gain horn antenna connected to a spectrum analyzer through two 22 dB gain and 3.5 dB noise figure low noise amplifiers. The measurement environment, an indoor hallway, is shown in Fig. 7. The received power of the modulated subcarrier (500 kHz modulation)—using measured spectra, such as the one shown in the inset of Fig. 8—was collected for increasing ranges up to 64 m, as shown in Fig. 8, and the measurements were

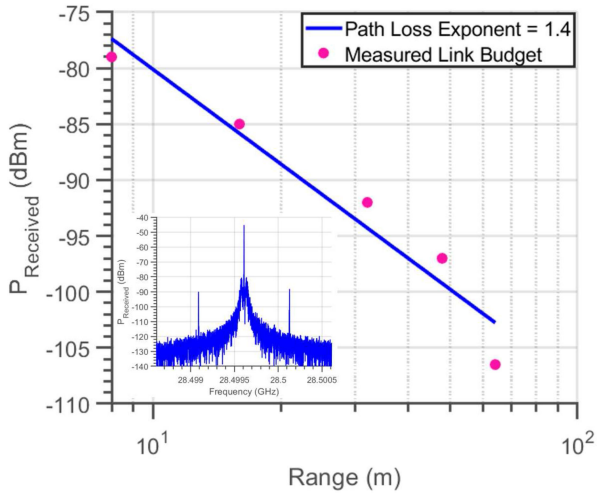

Fig. 8. Measured received power versus range and (onset) plot of one of the measured power spectra.

found consistent with a path loss exponent (PLE) of 1.4. This low exponent is consistent with what was reported in [12] for line-of-sight office-space configurations.

With a measured noise floor of -119 dBm at the 500 kHz offset and with a 2 kHz sampling rate, the measured signal to noise ratio at the maximum distance of 64 m was 12.5 dB. In such an environment and with this system, this would allow a maximum reading range of 179 m. It should be noted that the noise floor is here limited by the amount of phase-noise coupling from TX to RX measured to be around -70 dB. With 48 dBm EIRP, cross polarizing the response of the tag—a challenging task with the Rotman lens compared to Van Attas—and thereby allowing the cross polarization of the reader's TX and RX antennas could suffice to reduce the self-interference by the 22 dB required to reach the thermal noise floor. If one were to emit the full 75 dBm EIRP allowed by the regulations, the additional 27 dB of isolation could be achieved by combining analog, digital, and antenna techniques such as the one reported here [13]. In such conditions, maximum outdoor (with a PLE $=$ 2) ranges of 780 m and 1.8 km could be achieved with 48 dBm, and the 75 dBm maximum allowed for 5G base-stations EIRPs, respectively.

IV. Conclusion

In this letter, the Rotman lens—a passive type of BNFs—was used, for the first time, to realize a fully flexible autonomous RFID tag. The resulting system features unique characteristics such as high gain, wide angular coverage, and remarkable RCSs under both planar and bent conditions. The entire tag is powered with a small flexible solar cell operating under normal office lighting conditions. With those ground-breaking results, the Rotman-lens RFID tag has the potential of ultralong ranges up to 1.8 km under the maximum allowed EIRP transmitted power in the 5G band enabling the emergence of the first km-range retrodirective-enhanced RFIDs.

REFERENCES

[1] J. G. Hester and M. M. Tentzeris, "Inkjet-printed flexible mm-wave Van-Atta reflectarrays: A solution for ultralong-range dense multitag and multisensing chipless RFID implementations for IoT smart skins," *IEEE Trans. Microw. Theory Techn.*, vol. 64, no. 12, pp. 4763–4773, Dec. 2016.

[2] E. Sharp and M. Diab, "Van Atta reflector array," *IRE Trans. Antennas Propag.*, vol. AP-8, no. 4, pp. 436–438, 1960.

[3] J. G. Hester and M. M. Tentzeris, "A mm-wave ultra-long-range energy-autonomous printed RFID-enabled van-atta wireless sensor: At the cross-roads of 5G and IoT," in *Proc. IEEE MTT-S Int. Microw. Symp.*, 2017, pp. 1557–1560.

[4] J. A. Vitaz, A. M. Buerkle, and K. Sarabandi, "Tracking of metallic objects using a retro-reflective array at 26 GHz," *IEEE Trans. Antennas Propag.*, vol. 58, no. 11, pp. 3539–3544, Nov. 2010.

[5] B. R. Marshall, "Staggered pattern energy harvesting and retro-directive backscatter communications for passive RFID tags and sensors," Ph.D. dissertation, Georgia Inst. Technol., Atlanta, GA, USA, 2018.

[6] M. Alhassoun, M. A. Varner, and G. D. Durgin, "Theory and design of a retrodirective rat-race-based RFID tag," *IEEE J. Radio Freq. Identif.*, vol. 3, no. 1, pp. 25–34, Mar. 2019.

[7] M. S. Trotter, C. R. Valenta, G. A. Koo, B. R. Marshall, and G. D. Durgin, "Multi-antenna techniques for enabling passive RFID tags and sensors at microwave frequencies," in *Proc. IEEE Int. Conf. RFID*, 2012, pp. 1–7.

[8] A. Eid, J. Hester, and M. M. Tentzeris, "A scalable high-gain and large-beamwidth mm-wave harvesting approach for 5G-powered IoT," in *Proc. IEEE MTT-S Int. Microw. Symp.*, 2019, pp. 1309–1312.

[9] J. Kimionis and M. M. Tentzeris, "Pulse shaping: The missing piece of backscatter radio and RFID," *IEEE Trans. Microw. Theory Techn.*, vol. 64, no. 12, pp. 4774–4788, Dec. 2016.

[10] R. Rotman, M. Tur, and L. Yaron, "True time delay in phased arrays," *Proc. IEEE*, vol. 104, no. 3, pp. 504–518, Mar. 2016.

[11] J. D. Griffin and G. D. Durgin, "Complete link budgets for backscatter-radio and RFID systems," *IEEE Antennas Propag. Mag.*, vol. 51, no. 2, pp. 11–25, Apr. 2009.

[12] S. Sun *et al.*, "Investigation of prediction accuracy, sensitivity, and parameter stability of large-scale propagation path loss models for 5G wireless communications," *IEEE Trans. Veh. Technol.*, vol. 65, no. 5, pp. 2843–2860, May 2016.

[13] J. I. Choi, M. Jain, K. Srinivasan, P. Levis, and S. Katti, "Achieving single channel, full duplex wireless communication," in *Proc. 16th Annu. Int. Conf. Mobile Comput. Netw.*, 2010, pp. 1–12.